Haptic Links: Bimanual Haptics for Virtual Reality Using Variable Stiffness Actuation

Evan Strasnick[1] **Christian Holz[2]** **Eyal Ofek[2]** **Mike Sinclair[2]** **Hrvoje Benko[2]**

[1] Stanford University
Stanford, USA
estrasni@stanford.edu

[2] Microsoft Research
Redmond, USA
{cholz, eyalofek, sinclair, benko}@microsoft.com

Figure 1. (a) Three prototype Haptic Links attached to commercial HTC VIVE controllers. From left to right: *Layer-Hinge*, *Chain*, *Ratchet-Hinge*. (b-c) A survival game in which a Haptic Link rigidly locks handheld controllers in the shape of a two-handed gun. Overlay added in post-production for visualization.

ABSTRACT

We present Haptic Links, electro-mechanically actuated physical connections capable of rendering variable stiffness between two commodity handheld virtual reality (VR) controllers. When attached, Haptic Links can dynamically alter the forces perceived between the user's hands to support the haptic rendering of a variety of two-handed objects and interactions. They can rigidly lock controllers in an arbitrary configuration, constrain specific degrees of freedom or directions of motion, and dynamically set stiffness along a continuous range. We demonstrate and compare three prototype Haptic Links: *Chain*, *Layer-Hinge*, and *Ratchet-Hinge*. We then describe interaction techniques and scenarios leveraging the capabilities of each. Our user evaluation results confirm that users can perceive many two-handed objects or interactions as more realistic with Haptic Links than with typical unlinked VR controllers.

Author Keywords

Haptic Links; virtual reality; variable stiffness; haptics; two-handed; controller;

CHI 2018, April 21–26, 2018, Montreal, QC, Canada

ACM 978-1-4503-5620-6/18/04…$15.00
https://doi.org/10.1145/3173574.3174218

ACM Classification Keywords

H.5.1 [Information Interfaces and Presentation]: Multimedia Information Systems-Artificial, Augmented, and Virtual Realities; H.5.2 [User Interfaces]: Haptic I/O.

INTRODUCTION

Researchers have made significant advancements in the design of haptic controllers for virtual reality (VR), resulting in a variety of methods for rendering tactile and kinesthetic sensations in the hand [3,6,10,38]. However, the majority of this work prioritizes single-handed interactions, despite the prevalence of bimanual interactions in our lives [14]. That is, though many haptic controllers provide local feedback for a single hand interacting with an object, they cannot render forces *between* the hands. For example, when a user drives with a virtual steering wheel or swings a virtual golf club with handheld controllers, these interactions lack the physical constraints imposed by the real object.

In this paper, we focus not on the design of a VR haptic controller, but on *the design of a haptic connection between controllers*. We present Haptic Links, electro-mechanically actuated physical connections capable of rendering variable stiffness between two commodity handheld VR controllers. When attached, Haptic Links can dynamically alter the forces perceived between the user's hands to support the haptic rendering of a variety of two-handed objects and interactions. They can rigidly lock controllers in an arbitrary configuration, to, for example, make the controllers feel and behave like a two-handed tool or weapon (see Figure 1(c)). They can constrain specific degrees of freedom or directions of motion between the controllers, such as when turning a crank or pulling a lever. They can even set stiffness along a continuous range, to render friction, viscosity, or tension. In these ways, Haptic Links augment existing handheld controllers with realistic mechanical constraints, making interaction and game play in VR scenarios more immersive and tangible.

This paper presents the following contributions:

1. The design and implementation of three Haptic Link devices ("*Chain*," "*Layer-Hinge*," and "*Ratchet-Hinge*") enabling variable stiffness feedback between commodity handheld VR controllers;
2. Technical and user evaluations outlining the tradeoffs of each Haptic Link design and showcasing the potential of each in the haptic rendering of different object types;
3. Several two-handed interaction techniques and scenarios leveraging Haptic Links to improve bimanual haptic rendering in VR.

RELATED WORK

Haptic interfaces for VR interaction encompass a diverse set of devices and form factors. Wearable devices such as gloves and full-body suits present simulated tactile sensations to the skin, often utilizing vibrotactile or electrical feedback [12,20,50]. Exoskeleton-type devices are similarly worn, but mechanically impart forces or constrain motion around the fingers, hands, or arms to render haptic sensations on a variety of scales and resolutions [5,11,42,44]. Because they do not require the user to hold a device, both wearables and exoskeletons free the user's hands and fingers for direct interactions with the virtual environment.

Another widely studied class of haptic system is the actuated force-feedback arm, such as the PHANToM family of devices [16,23,26,29]. These arms typically make use of a grounded physical reference in the user's environment. As a result, they can impart net forces on the user to render large haptic forces and collisions, but often at the cost of reduced mobility and operating space. In contrast, encountered-type devices such as robotic arms and drones [2,47] follow the user as they move through the environment, making physical contact as needed to render haptic cues. Though they offer mobility and support large interaction spaces, challenges in predicting and reacting to the user's movements often result in issues of latency.

More recently, another form factor—the handheld controller—has emerged as the dominant mode of interaction in consumer VR systems, such as in the Oculus Rift [30] and the HTC VIVE [17]. Though handheld controllers greatly simplify the tracking and input requirements of VR systems, their haptic capabilities are frequently limited to integrated vibrotactile motors. They may also include physical inputs which provide passive feedback, such as triggers, buttons, and joysticks. Recent work has targeted the controller form factor in enabling rich haptic interactions such as touch, grasping, weight, and texture [3,9,10].

Bimanual Haptics in VR

Despite the range of technologies capable of rendering haptic sensations on the hands in VR, systems that provide feedback *between* the hands are less widely studied. Typical bimanual tasks vary greatly in the positioning, orientation, and relative motion of the hands [14]. The increased distances, stronger forces, and numerous degrees of freedom in bimanual scenarios make many conventional haptic solutions infeasible. Grounded force-feedback systems, described above, can support bimanual feedback when used in pairs by rendering forces on each manipulandum in a coordinated manner [32,41]. Such dual articulated arm setups are most frequently used in cases of robotic telemanipulation [18,21] or in surgical simulation [7,24], where precise bimanual actions are crucial. However, the size, cost, and complexity of these setups prohibit their widespread usage with commodity VR systems.

An alternative solution uses *passive* controller augmentations to improve the haptic presentation of a *specific* virtual object. For example, a number of commercially sold attachments anchor VR controllers in the form factor of a two-handed gun, enabling users to feel realistic handling in applications that utilize rifles or other such weapons [34,44]. Similar attachments exist for golf clubs [45], musical instruments [31], and more. Though simple and compelling, these passive attachments are static, making them less effective for rendering multiple types of objects, or objects that are deformable or customizable.

Variable Stiffness Feedback

We consider variable stiffness actuation as a possible mechanism by which to enable general-purpose bimanual feedback in VR. Variable stiffness as a feedback technique is well studied. Approaches include electromechanical actuators, jamming, rheological fluids, shape memory alloys (SMAs), and low-melting point alloys. Detailed reviews of these techniques can be found in [25] and [43].

Already, researchers have applied several of these variable stiffness techniques in the design of haptic interfaces. Mechanical exoskeletons utilize belts and cables to stiffen individual joint motion [42]. Wearable interfaces have employed jamming to restrain finger movements in a glove-type form factor [39], as well as in the design of full-limb restraints [27]. Similarly, MR fluid brakes have been used in the design of a haptic glove for VR [4]. Other researchers have leveraged shape-memory alloys and electromechanical approaches to enable variable stiffness interactions with mobile devices [15,28]. The Haptic Links described in this paper apply these variable stiffness actuation techniques on a larger scale to dynamically brake the relative motion between two handheld controllers.

DESIGN AND IMPLEMENTATION

The implementation of our Haptic Link vision began with numerous design considerations. These included: stiffness when actuated, flexibility when relaxed, resolution of stiffness, weight, bulk, moment of inertia, actuation speed, power consumption, noise, and range of motion. The ideal Haptic Link would be virtually undetectable to a user prior to actuation, but could stiffen quickly, strongly, and precisely as needed.

Of the studied approaches for rendering variable stiffness, we first ruled out both SMAs and low-melting point alloys, which have prohibitively long actuation periods, and ER/MR fluids, whose solutions tend to settle out over time leading to decreasing effectiveness. Particle jamming interfaces showed promise with relatively high stiffness gains, particularly when reinforced with internal frames or skeletons [8,27,46]. However, such reinforcements reduce the flexibility of the joint when unjammed, and the volume of matter required adds significant weight to the mechanism. Layer jamming was perhaps more promising, as researchers have successfully used it to produce light, flexible manipulators with significant stiffening capabilities [19,37]. However, for both jamming techniques, actuation remained unsuitably slow, and the large pumps required ultimately led us to focus on electro-mechanical stiffening approaches.

Existing electromechanical techniques to produce variable stiffness could easily achieve sufficiently high braking torques as well as quick and precise stiffness control. However, due to the size, weight, and power constraints of our task, using motors and brakes to directly oppose the user's torque quickly became infeasible. Thus, our designs shifted to investigate alternative joints and mechanisms which could be indirectly actuated using smaller motors.

Our exploration yielded three prototype Haptic Links (Figure 1(a)), all capable of allowing and halting the 6-DOF motion of handheld VR controllers. Each design has tradeoffs and advantages over the others, making them best suited for different applications. We envision that designers of VR experiences could choose the Haptic Link that best meets their needs out of many options, allowing users to quickly attach the recommended Haptic Link to their controllers prior to entering the virtual world.

We chose to design our Haptic Links to fit the commercially available HTC VIVE [17] controllers, due to the ease of constructing mounting geometries either for the annular tracking region or the protruding base. All Haptic Links affix to these controllers without additional modifications. Each Haptic Link connects via ribbon cable to a regulated power supply and to a Teensy 3.2 microcontroller [33] which controls the actuators on the device. VR applications can communicate with this controller via serial to dynamically update the stiffness of each joint in the Haptic Link. Both our VR experiences and our user evaluation were implemented in the Unity 2017 game engine.

Chain Device

The *Chain* prototype (Figure 2), utilizes a highly articulated chain composed of ball-and-socket elements. A strong cable is threaded through the length of the chain and tethered to a linear actuator on each end. With the linear actuators extended, the chain is kept loose such that the user can arbitrarily move the controllers in 3D space. When the linear

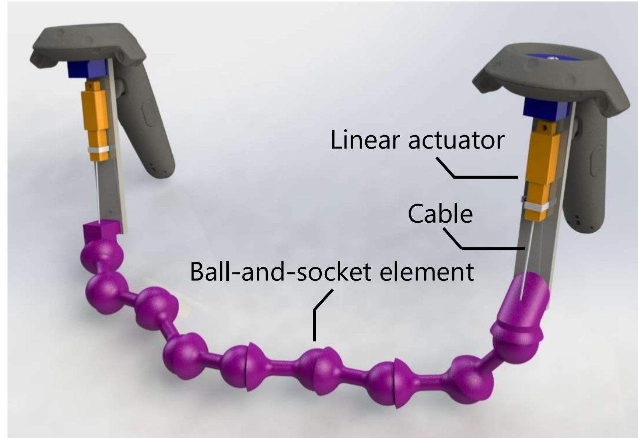

Figure 2. The *Chain* prototype stiffens an articulated chain by pulling tight a cable threaded through ball-and-socket elements.

actuators retract the cable, the ball-and-socket elements are compressed into one another, increasing the friction at each joint in the chain. As a result, the entire chain stiffens, fixing the current spatial relationship between the two controllers.

The *Chain* prototype uses two Actuonix L12-R Micro Linear Servos [1] each capable of 80 N maximum force at 6.5 mm/s. The ball-and-socket elements were 3D printed using a PolyJet material, and the cable is an ultra-high-molecular-weight polyethylene string (1 mm diameter, 160 kg breaking force, 4.8% breaking elongation). The linear servos are mounted onto laser cut Polyoxymethylene pieces and oriented coaxially with the ends of the chain. Each of these pieces then mounts onto two 3D printed conical frusta which clamp down on either side of the annular portion of the HTC VIVE controller.

The *Chain* prototype was designed for unrestricted 6-DOF motion which can globally stiffen in any configuration. Though it can render non-binary stiffness, precise control over the intermediate range is difficult, as stick-slip motion between the individual elements results in a nonuniform perception of stiffness. Models of the frictional forces in the interdependent ball-joint elements are beyond the scope of this paper, but details can be found in [37].

Layer-Hinge Device

The second prototype (*Layer-Hinge*, Figure 3) consists of two main components: ball joints to allow rotation of the controllers, and a hinge controlling the distance between them. Each controller is connected at its base via a 3D printed mount to a ball joint capable of 360° pan and 60° tilt rotation. A FEETECH FS5115M servo [13] (180° rotation in .48 s, 15.5 kg-cm torque) drives the set screw on each ball joint, locking and unlocking rotation of the controller. The hinge component consists of a series of interleaved layers of laser cut cast acrylic. An additional FS5115M servo drives a bolt threaded through the layers and a captive nut on the other end. As the nut cannot rotate,

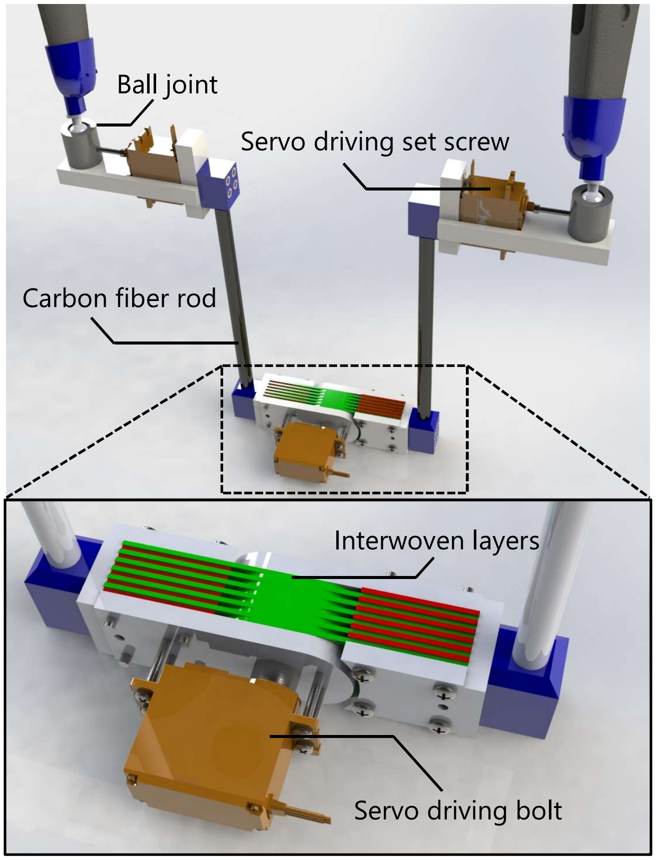

Figure 3. The *Layer-Hinge* prototype consists of locking ball joints to control rotation and a hinge leveraging the friction between layers to control distance between controllers.

the rotational motion of the bolt compresses the layers, increasing the overall friction of the hinge based on the number of layers in contact. The hinge and ball joint pieces are connected by carbon fiber rods (21.5 cm length, 1.27 cm diameter).

With three distinct points of actuation, the *Layer-Hinge* prototype has the advantage of selectively locking individual degrees of freedom in the motion of the controllers. For example, if the hinge is locked but the ball joints remain free, the controllers can rotate at a fixed distance apart, much like joysticks. Further, the friction of each joint can be controlled with relative precision, allowing the device to render a continuous range of stiffness values in both the hinge and ball joints. The resistive force in the hinge can be modeled with the relationship

$$F = \mu n p A$$

where μ is the static coefficient of friction of the cast acrylic, n is the number of contact layers (12), p is the applied pressure, and A is the contact area of each layer.

Ratchet-Hinge Device

The third prototype (*Ratchet-Hinge*, Figure 4) uses the same ball joint components beneath the controllers as in the *Layer-Hinge* prototype, but replaces the hinge with a dual-

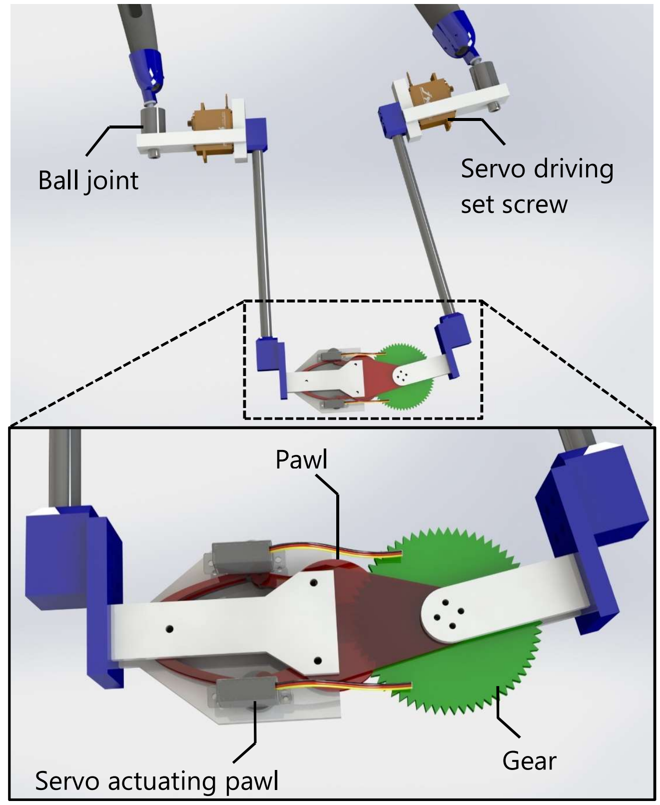

Figure 4. The *Ratchet-Hinge* prototype uses locking ball joints and a dual-ratchet hinge. Each of the opposing pawls can be individually disengaged to control both directions of motion.

ratchet mechanism capable of independently braking inward or outward motion. The ratchet mechanism is cut from Polyoxymethylene and features two pawls set against a central gear at opposite angles. A Hitec HS-35HD Nano Servo [36] with an attached cam disengages each pawl, freeing the corresponding direction of motion. With both pawls engaged, the gear is fixed, and with both disengaged, the gear can rotate freely. When one pawl is disengaged, the gear can ratchet against the engaged pawl in one direction, but rotation in the opposite direction further engages the remaining pawl and halts the motion.

The directionally-selective capabilities of the *Ratchet-Hinge* prototype enable unique force-feedback interactions, such as the rendering of a midair impassable surface. However, each ratchet can only engage or disengage in a binary fashion, and thus the prototype trades away the intermediate stiffness capabilities of the *Layer-Hinge* prototype.

TECHNICAL EVALUATION

Table 1 compares the technical specifications of each Haptic Link, and Figure 5 shows experimentally obtained torque-angle curves of the prototypes when fully stiffened. Torque-angle measurements were taken using a lathe by anchoring one end of the joint to the spindle, attaching the other end in series with a force gauge to the slide, and recording measurements while stepping back the slide (Figure 6). Measurements were taken with the arms of the proto-

	Chain	*Layer-Hinge*	*Ratchet-Hinge*
Weight (g) (without controllers)	673	793	651
Weight distribution	Evenly distributed	Concentrated at the base of the controllers and at the hinge	Concentrated at the base of the controllers
Actuation speed (s) (0-100%)	1.0	Hinge: .65, Ball Joint: .50	Hinge: .13, Ball Joint: .50
Maximum distance between controllers (cm)	54	63	68
Stiffness control	Continuous	Continuous	Binary

Table 1. Technical specifications of each Haptic Link prototype.

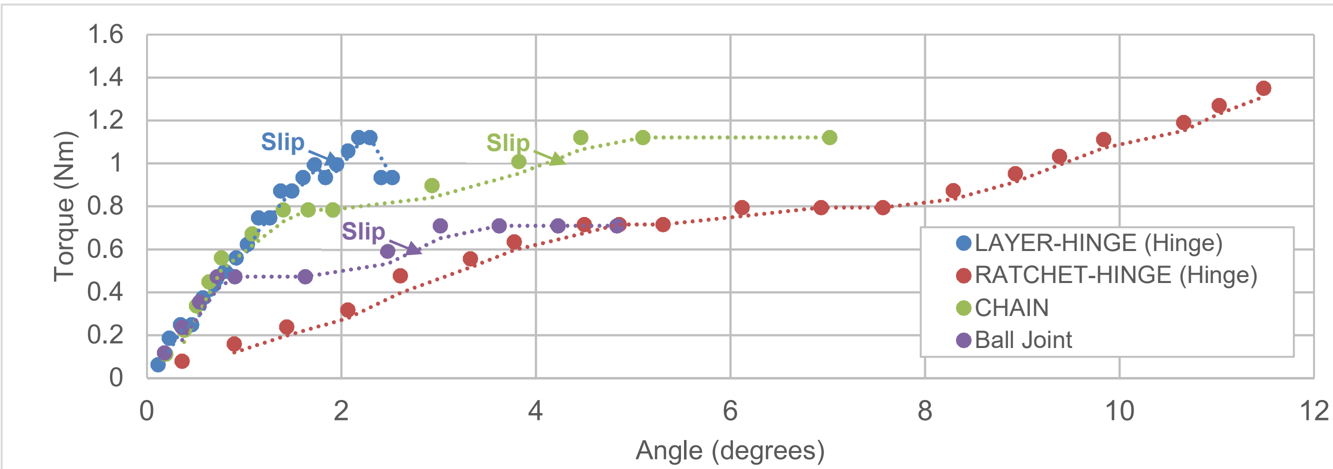

Figure 5. Torque-angle curves for each actuated component of the prototypes. The Ball Joint curve applies to both the *Layer-Hinge* and *Ratchet-Hinge* prototypes. The hinge of the *Ratchet-Hinge* was not driven to failure (due to its having a critical failure mode), whereas all other components were driven until torque remained constant.

types parallel to each other and perpendicular to the applied force. Both the *Chain* prototype and the hinge of the *Layer-Hinge* prototype reached maximum torques of 1.1 Nm before slippage, whereas the ball joints used in the *Layer-Hinge* and *Ratchet-Hinge* prototypes yielded only .7 Nm. The hinge of the *Ratchet-Hinge* prototype holds until mechanical failure of the ratchets. Due to our having only a single Haptic Link of each design, we did not test destructive failure modes.

The prototypes can be configured to operate in a power-efficient mode or to optimize for the maximum possible stiffness. For most purposes, the actuators can be set such that the static back drive force is used to hold the joint when fully stiffened. In this case, power exceeds the standby power (.05-.1W) only when moving the servos (i.e. changing the stiffness). This transient consumption varies based

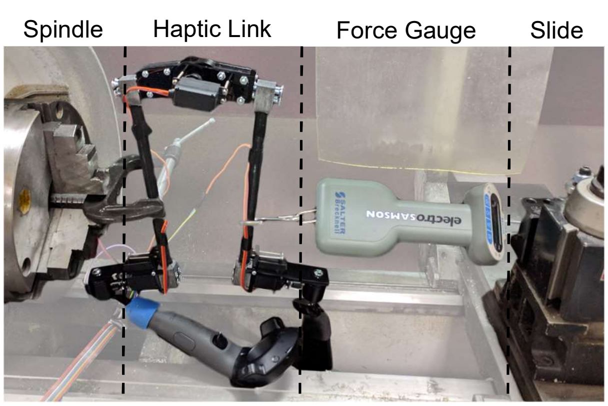

Figure 6. Setup for measuring Torque-angle curves on a lathe.

on the stiffness of the joint, but ranges from 1-5 W on each prototype. In addition, we can instead configure the Haptic Links to push the maximum stiffness further by holding at stall torque. In this case, the total power consumption depends upon the time spent at maximum stiffness, for which the stall power consumption is around 4.8-7.2 W on all prototypes. The motors may grow warm if left at stall for significant periods, though no heat-related issues were ever detected during the course of this work.

USER EVALUATION

We designed an evaluation to investigate the following questions:

1. Can inter-controller variable stiffness feedback contribute to a more realistic haptic rendering for two-handed objects and interactions than that of conventional (unlinked) controllers?
2. Which of the Haptic Link prototypes are most effective in providing realistic haptic renderings for different types of objects?

Methodology

We recruited 12 participants from our organization (ages 25-49, 1 female) to help in answering these questions. Participants were asked to rate their perceptions of object realism using each Haptic Link and a control pair of unlinked HTC VIVE controllers. For each trial, participants first aligned their controllers into the proper positions for the object using visual indicators. Once correctly positioned,

Figure 7. Objects explored in the user evaluation. Left to right, top to bottom: RIFLE, BOW, TROMBONE, PISTOLS. Overlay added in post-production for visualization.

the virtual controller models disappeared and were replaced by the target object. Haptic rendering then began, and the participant was allowed up to 30 seconds to freely explore the object. Once finished exploring, the participant responded to the following question on a 1-5 Likert scale: "How much did it feel like you were holding and handling a real object?" The participant selected a response using a laser pointer tool, and then continued to the next trial.

We presented four objects (described below) across four device conditions (*Chain*, *Layer-Hinge*, *Ratchet-Hinge*, and unlinked VIVE controllers). Each participant explored each object twice on each condition, for a total of 32 trials. Trials were grouped into device blocks, such that participants explored all objects in one device condition before switching to another device. The order of object presentation was randomized within a device block, and device blocks were counterbalanced across participants.

After each device block, participants rated aloud qualitative aspects of the current device by agreeing with statements on a 1–5 scale (1 = "Strongly disagree", 5 = "Strongly agree"). The aspects rated were comfort ("I found the controllers comfortable to use") and movability ("I found that I could move the controllers as desired or expected").

To prevent the effects of visual bias on the ratings of any device condition, participants did not see any of the controllers until the end of the study. The devices were hidden prior to the arrival of the participant, and participants kept on the HMD throughout the study as devices were taken from and placed into their hands. Participants wore headphones playing brown noise to prevent listening for any noises from motor activations.

Virtual Objects

We presented participants with the following four virtual objects (Figure 7). These objects were selected to cover a range of possible stiffness requirements and motion types, to fully explore the capabilities of each Haptic Link. Table 2 describes how stiffness was applied to each Haptic Link to render these objects. Standard vibrotactile feedback on the unmodified VTVE controllers was used across all objects and conditions. We refer the reader to the accompanying Video Figure to see these objects in greater detail:

- RIFLE: A two-handed rifle was rendered such that the participant's right hand held the trigger, while their left hand rested beneath the forestock.
- BOW: A recurve bow and arrow were rendered such that the participant's left hand held the bow at its grip while the right hand held an arrow. After setting the arrow in the bow's nock, the participant held the trigger while retracting their right hand to pull back the bowstring and arrow. Releasing the trigger fired the arrow. Slight vibrations were felt while pulling back the bowstring.
- TROMBONE: A trombone was rendered such that the bell section was held in the left hand while the right hand held the slide. Moving the right hand towards and away from the left hand controlled the motion of the virtual slide. The slide would not move past its first position (too close) or beyond the end of the tubing (too far)

	Chain	*Layer-Hinge*	*Ratchet-Hinge*
RIFLE	Rigidly locked	Rigidly locked	Rigidly locked
BOW	Increasing stiffness as the user draws bow	Left (bow hand) ball joint locked; increasing stiffness as the user draws bow	Left (bow hand) ball joint locked; outward motion braked when fully drawn
TROMBONE	Small baseline stiffness	Small baseline stiffness in hinge; ball joints locked	Ball joints locked; directional brake as user exceeds max/min slide
PISTOLS	Unlocked	Unlocked	Unlocked

Table 2. Specific stiffness applied to each Haptic Link to render the objects in the user evaluation.

to prevent unrealistic renderings or separation of the pieces. Slight vibrations were felt as the slide moved.

- PISTOLS: Two pistols were rendered to track each of the participant's controllers individually.

Hypotheses

The RIFLE served to inform whether Haptic Links improve the realistic presentation of rigid two-handed objects. The BOW primarily explored dynamically increasing stiffness values in a continuous range (for applicable Haptic Links). The TROMBONE investigated constrained degrees of freedom in motion as well as directionally selective braking (for applicable Haptic Links). Finally, the PISTOLS served as a control condition to determine whether the presence of the Haptic Link detracts from the haptic presentation of otherwise disjoint objects.

Thus, for each object, post-hoc comparisons were made between each Haptic Link condition and the unlinked VIVE controllers. In particular, the Haptic Links were hypothesized to be perceived as more realistic in the RIFLE, BOW, and TROMBONE conditions, and less realistic in the PISTOLS condition.

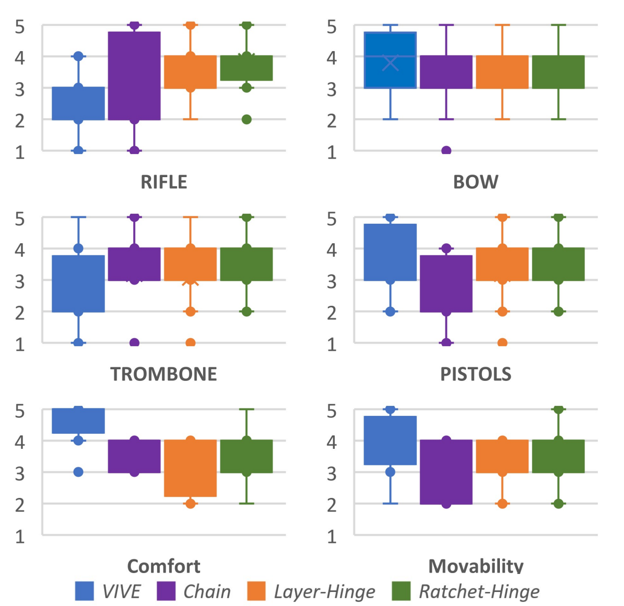

Figure 8. Box plots aggregating object-device realism ratings and overall device ratings.

Results and Discussion

Figure 8 and Table 3 summarize the ratings for each device-object combination, as well as overall comfort and movability responses from post-device feedback. Using Wilcoxon Signed-Ranks Tests, we assessed the comparisons between each Haptic Link and the unlinked VIVE controllers for each condition. We used Dunnett's Test as a follow-up measure to account for multiple comparisons against the control group.

Participants considered all Haptic Links to be significantly more realistic than unlinked controllers for the RIFLE object, suggesting that variable stiffness haptics can indeed improve the haptic rendering of rigid two-handed objects.

Mean ratings were also higher for all Haptic Links with the TROMBONE but failed to reach adjusted statistical significance. Ratings were highest for the *Ratchet-Hinge* proto-

	VIVE	***Chain***	***Layer-Hinge***	***Ratchet-Hinge***	**χ-crit**
RIFLE	2.75	3.54 ***p* = .017***	3.57 ***p* = .005***	3.83 ***p* = .001***	.67
BOW	3.79	3.54 *p* = .314	3.65 *p* = .367	3.71 *p* = .528	.64
TROMBONE	2.75	3.21 *p* = .098	3.08 *p* = .235	3.38 ***p* = .020**	.73
PISTOLS	3.63	2.83 ***p* = .026***	3.21 *p* = .100	3.63 *p* = .973	.68
Overall Comfort	4.7	3.7 ***p* = .003***	3.2 ***p* = .003***	3.3 ***p* = .005***	.7
Overall Movability	3.9	3 ***p* = .042***	3.3 *p* = .086	3.7 *p* = .594	.9

* = Significance persists following multiple comparisons adjustment using Dunnett's test (minimum significant distance between group means listed as **χ-crit**)

Table 3. Mean ratings and p-values for object-device realism and overall device ratings. p-values represent comparisons to unlinked VIVE controllers within the same category.

type, which is expected given that it was the only prototype capable of rendering the outward stop matching the end of the range of motion of the visual slide component.

The results from the BOW trials are more surprising, as ratings were similar across all conditions. Follow-up interviews with participants indicated that they were highly sensitive to the nuances of each Haptic Link's motion in the context of such a complex action. Among the issues noted were the lack of a true spring force in the bowstring, the time to fully release stiffness after firing, and the inability to pull straight back on the hinged devices while holding the bow upright. In contrast, when using the unlinked controllers, participants rarely critiqued the experience at all, despite the complete lack of feedback between the bow and bowstring. One possible conclusion is that users are more willing to accept no feedback in the rendering of an object (perhaps due to familiarity) than *incorrect* feedback.

Finally, only the *Chain* prototype had significantly lower ratings than the unlinked controllers for the PISTOLS object. Participants largely attributed these sentiments to a limited range of motion due to the chain's length.

Participants rated comfort as significantly higher for the unlinked controllers than for the Haptic Links. Weight was the most frequently mentioned issue, as well as the feeling that the Haptic Link could be felt protruding if the controllers were held close and at a particular angle. However, some participants noted that despite the impact on comfort, the added weight improved the realism of the virtual objects. Others specifically mentioned that the linked controllers felt less familiar in their hands, which suggests a follow-up evaluation with longitudinal design to explore the effects of familiarity. Finally, Movability ratings were significantly decreased only for the *Chain* prototype. As highlighted during the PISTOLS trials, the shorter length of the *Chain* prototype resulted in an unsatisfactory range of motion for scenarios requiring total freedom of each controller.

Given these results, we can begin to consider guidelines for designers that suggest the usage of different Haptic Links for different objects and interactions. For example, both the *Layer-Hinge* and *Ratchet-Hinge* models are effective in switching between objects that require rigid locking and free motion, such as picking up and wielding various static objects. While the *Chain* device suffers from a decreased effective length and slower actuation speed, it can be freely positioned in different shapes and is safe to grab, having no exterior actuated elements along the chain. Thus, we might suggest its use in wheels, levers, ropes, and other arbitrarily-shaped tools that users can grasp in different positions.

APPLICATIONS AND EXTENSIONS

Along with user evaluation, we explored the potential of our Haptic Link attachments for supporting richer bimanual interactions in VR through several techniques.

Figure 9. Summoning a vehicle using gestural input (left), then driving with a rigid steering wheel (right).

Object Summoning

As our Haptic Links can currently only provide resistive forces (that is, they cannot actively move controllers into a given configuration), a key question is how to get the user's controllers positioned appropriately to render a particular object. Similar to existing work leveraging gestures that mimic physical input [40], our first approach—referred to as "Summoning"—allows the user to assume a desired object at will by mimicking its shape with their controllers. We explored this technique in the context of a virtual racing game (Figure 9), where the user can Summon either a car or a motorcycle around them by placing their controllers in the shape of a steering wheel or handlebars respectively. Once in position, the Haptic Link rigidly locks the controllers, thus rendering the steering wheel/handlebars which the user can rotate as if steering a real vehicle. By pressing a button on the controller, the Haptic Link relaxes, and the vehicle disappears. With this technique, users can easily switch between objects on the fly by Summoning them through the correct pose of the two controllers.

In a similar fashion, we also created a zombie shooter game utilizing the rifle and dual pistol weapons featured in the user study (Figure 1(b-c)). By default, players can shoot pistols in each hand, but by holding their hands out as if wielding a rifle, the pistols are replaced by the rifle weapon, which shoots farther and faster. Upon transition, the Haptic Link rigidly locks the controllers in the rifle configuration. A button on the controller returns to the pistols, allowing the user to switch between weapons at will. Through Summoning, Haptic Links allow users to wield an indefinite number of objects with different haptic presentations.

Object Retrieval Indicators

With Summoning, the user can take up a given object at any time—as if the object is always with them. An alternative style of interaction is manual object acquisition: the object exists in a particular location and the user must approach and pick it up. To ensure that the controllers are properly arranged for haptic rendering in this style of interaction, we use a set of visual indicators that represent the proper position and orientation of each controller to pick up the object.

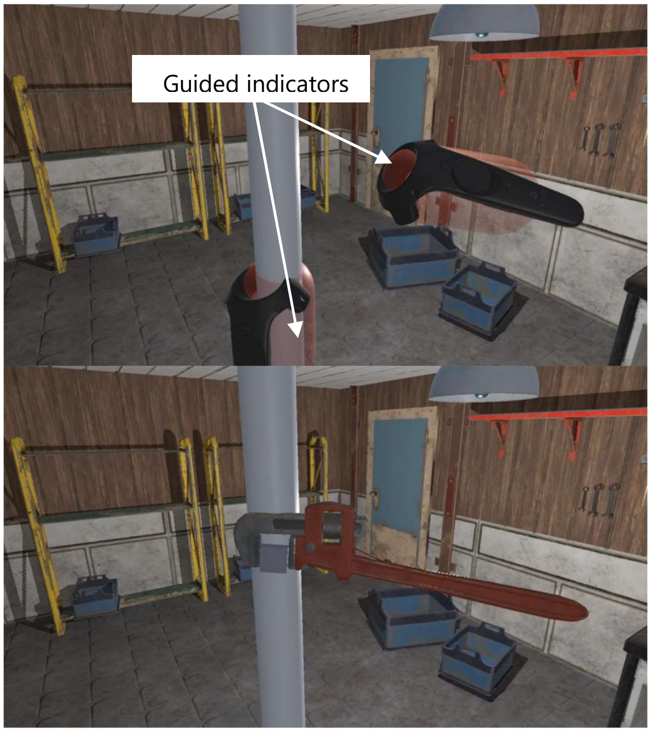

Figure 10. Using guided indicators (top) to retrieve a wrench object (bottom).

We created a plumbing scenario (Figure 10) demonstrating the use of these indicators, in which users tighten down a nut on a pipe using a wrench. One controller holds the wrench while the other holds the pipe. To begin the interaction, the user must approach the pipe, grab the pipe below the nut with one hand, and position their other hand at the highlighted zone in the air above the nut. When correctly positioned, the wrench appears, and the Haptic Link provides increasing stiffness on the downswing, while releasing the stiffness as the user returns on the upswing.

Grasping Virtual Objects

By tracking the controllers and locking them in a directionally-selective fashion as they move through virtual space, the *Ratchet-Hinge* prototype can render impassable virtual surfaces. We explored this capability in the context of two-handed grasping interactions by creating a virtual playground where users grasp objects of different sizes between their hands (Figure 11).

Controller Grounding

Again leveraging the directional capabilities of the *Ratchet-Hinge* prototype, we can anchor one controller to a fixed point, and then using the Haptic Link to provide grounded force feedback to the other: In short, the user grounds either on-body (the user anchors a controller to their body) or externally (the user anchors a controller to a fixed surface in the room). Then, we can repurpose the variable stiffness actuation of the Haptic Link to halt motion of the remaining controller in the user's hand. For example, if the user grounds one controller at their waist, we can render solid walls and objects by braking outward motion of the controller as it contacts each surface. We fabricated an additional controller mount allowing one of the linked controllers to attach either on-body or externally (Figure 12), and then designed a virtual environment where users could reach out and explore walls in front of them.

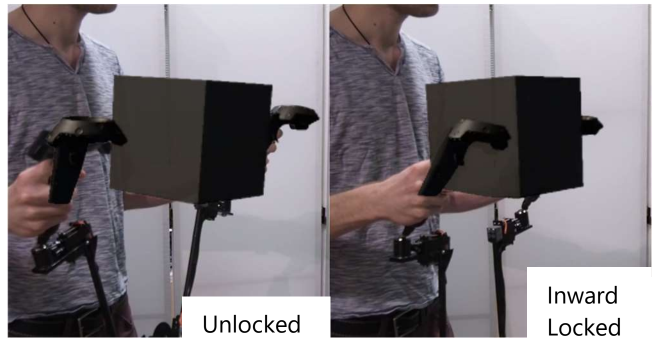

Figure 11. Using directionally-selective braking to grasp objects with two hands. As the controllers meet the object, inward motion is braked. Overlay created using post-processing.

Figure 12. Grounding one controller at the waist (top) or on an external surface (bottom), to enable grounded force-feedback interactions with the other controller via the Haptic Link.

LIMITATIONS AND FUTURE WORK

Despite the capabilities we have shown, the Haptic Link prototypes have limitations requiring further iteration. From a mechanical standpoint, users mentioned weight, bulk, and range of motion as noticeable detractors, all of which can be improved through modifications to the design, materials, and fabrication. As our prototypes were primarily built with laser cut or 3D printed components, switching to manufactured components should improve not only weight and sturdiness, but precision and robustness of the friction-based mechanisms as well. Additional investigation is needed to fully understand the ergonomic impacts of Haptic Links, such the added moment of inertia in different controller poses, motion constraints given different sizes and attachment sites of the Haptic Link, as well as potential muscle fatigue from extended use.

From an actuation standpoint, the maximum stiffness of most joints—though enough to present rigidity to the user—can be overcome through the user's full strength. Similarly, some users noted that a faster speed of actuation could improve the rendering of quick transitions—for example, the releasing of tension on the bowstring. We can improve both the maximum braking torque and the actuation speed by using more performant motors and by iterating on the designs of our joint mechanisms. However, our results also suggest the need for further evaluation to identify how much—or how little—stiffness is needed to perceive the controllers as a unified object, and how quickly actuation must occur to render compelling interactions.

Finally, several modifications could make Haptic Links more convenient for use with a commodity VR setup, such as making them adjustable in length, removing the need for a wired connection, and creating an attachment mechanism that allows them to quickly snap onto and off of the controllers. Longevity of the friction-based mechanisms is also a concern: over the course of our development and evaluation, we occasionally found the need to recalibrate the motors to adjust for wear in the frictional surfaces.

More generally, the resistive nature of Haptic Links limits the range of possible types of force feedback that they can present. Specifically, Haptic Links cannot provide inertial force feedback, meaning that while they can introduce forces between the hands, they cannot impart net forces onto them. Further, Haptic Links are incapable of rendering the spring forces found in many objects. If stiffness is applied as a controller moves in one direction, there is no restoring force in the opposite direction. Future Haptic Links could include additional components such as gyroscopic mechanisms or springs to render such forces, and designers could choose these Haptic Links as needed by their VR scenarios.

Beyond improvements to the devices themselves, we aim to explore as future work how Haptic Links can influence the perception of other haptic techniques and phenomena in bimanual scenarios. For example, recent work has examined illusory haptics in VR [22,35], finding that the vibrotactile feedback in most handheld controllers can be leveraged to present stimuli that seem to originate from different locations on a virtual object held between the hands. As our results show that users can perceive a two-handed object more realistically with a Haptic Link, we can investigate whether the Haptic Link also improves the robustness of these spatio-haptic illusions. We can also explore the power of visual dominance in expanding the capabilities of Haptic Links. For example, can a sufficiently visually compelling experience lead users to perceive spring forces or inertial forces that cannot be rendered by the Haptic Link? Or, by effectively redirecting users' focus and movement, can we design the interaction such that the users themselves provide these forces from the other controller? We find these open questions to be exciting future work as we continue to iterate on the design of our Haptic Links.

CONCLUSION

Haptic Links demonstrate the potential to improve the haptic rendering of two-handed objects and interactions in VR using inter-controller variable stiffness feedback. The multiple implementations of Haptic Links yield different capabilities and advantages for object rendering. Our evaluation shows that Haptic Links can improve the perceived realism of two-handed objects without significantly detracting from the rendering of normal interactions requiring disjoint controllers. Finally, the interaction techniques we introduce leverage Haptic Links to provide more compelling haptic experiences in VR.

Virtual reality has become increasingly immersive, leaving us with a growing need for authentic haptic interactions. Haptic Links offer designers of VR experiences a wide range of new haptic tools that work seamlessly with the handheld controllers of commodity VR systems. While our prototypes represent just a starting point in the design of future Haptic Links, we find their early success encouraging for the exploration of a new class of devices which can rapidly augment existing controllers to provide a customized haptic experience.

REFERENCES

1. Actuonix. 2017. L12-R Micro Linear Servos for RC & Arduino. Retrieved January 1, 2017 from https://www.actuonix.com/L12-R-Linear-Servo-For-Radio-Control-p/l12-r.htm
2. Bruno Araujo, Ricardo Jota, Varun Perumal, Jia Xian Yao, Karan Singh, and Daniel Wigdor. 2016. Snake Charmer. In *Proc. TEI 2016*, 218–226. https://doi.org/10.1145/2839462.2839484
3. Hrvoje Benko, Christian Holz, Mike Sinclair, and Eyal Ofek. 2016. NormalTouch and TextureTouch. In *Proc. UIST 2016*, 717–728. https://doi.org/10.1145/2984511.2984526
4. Jonathan Blake and Hakan B. Gurocak. 2009. Haptic glove with MR brakes for virtual reality. In *IEEE/ASME Transactions on Mechatronics* 14, 5: 606–615. https://doi.org/10.1109/TMECH.2008.2010934
5. M Bouzit, G Burdea, G Popescu, and R Boian. 2002. The Rutgers Master II-ND Force Feedback Glove. In *Proc. HAPTICS 2002*, 256–263. https://doi.org/10.1109/HAPTIC.2002.998952
6. Tom Carter, Sue Ann Seah, Benjamin Long, Bruce Drinkwater, and Sriram Subramanian. 2013. UltraHap-

tics : Multi-Point Mid-Air Haptic Feedback for Touch Surfaces. In *Proc. UIST 2013*, 505–514. https://doi.org/10.1145/2501988.2502018

7. Sonny Chan, François Conti, Kenneth Salisbury, and Nikolas H. Blevins. 2013. Virtual Reality Simulation in Neurosurgery. In *Neurosurgery* 72, January: A154–A164. https://doi.org/10.1227/NEU.0b013e3182750d26
8. Nadia G. Cheng, Maxim B. Lobovsky, Steven J. Keating, Adam M. Setapen, Katy I. Gero, Anette E. Hosoi, and Karl D. Iagnemma. 2012. Design and analysis of a robust, low-cost, highly articulated manipulator enabled by jamming of granular media. In *Proc. ICRA 2012*, 4328–4333. https://doi.org/10.1109/ICRA.2012.6225373
9. Inrak Choi, Heather Culbertson, Mark Roman Miller, Alex Olwal, and Sean Follmer. 2017. Grabity: A Wearable Haptic Interface for Simulating Weight and Grasping in Virtual Reality. In *Proc. UIST 2017*, 199-130. https://doi.org/10.1145/3126594.3126599
10. Inrak Choi and Sean Follmer. 2016. Wolverine: A Wearable Haptic Interface for Grasping in VR. In *Adjunct Proc. UIST 2016*, 117–119. https://doi.org/10.1145/2984751.2985725
11. CyberGlove Systems Inc. 2017. CyberGrasp Glove. Retrieved January 1, 2017 from http://www.cyberglovesystems.com/cybergrasp/
12. CyberTouch. 2017. CyberTouch Glove. Retrieved January 1, 2017 from http://www.cyberglovesystems.com/cybertouch/
13. FeeTech. 2013. Standard 15kg.cm Metal Gears Analog Servo FS5115M. Retrieved January 1, 2017 from http://www.feetechrc.com/product/analog-servo/standard-15kg-cm-metal-gears-analog-servo-fs5115m/
14. Yves Guiard. 1987. Asymmetric Division of Labor in Human Skilled Bimanual Action. In *Journal of Motor Behavior* 19, 4: 486–517. https://doi.org/10.1080/00222895.1987.10735426
15. Sidhant Gupta, Tim Campbell, Jeffrey R. Hightower, and Shwetak N. Patel. 2010. SqueezeBlock: Using virtual springs in mobile devices for eyes-free interaction. In *Proc. UIST 2010*, 101-104. https://doi.org/10.1145/1866029.1866046
16. Haption SA. 2017. Haption Virtuose 6D. Retrieved January 1, 2017 from https://www.haption.com/site/index.php/en/products-menu-en/hardware-menu-en/virtuose-6d-menu-en
17. HTC. 2017. Vive. Retrieved January 1, 2017 from https://www.vive.com/us/product/vive-virtual-reality-system/
18. O Khatib, X Yeh, G Brantner, B Soe, B Kim, S Ganguly, H Stuart, S Wang, M Cutkosky, A Edsinger, P Mullins, M Barham, C R Voolstra, K N Salama, M L'Hour, and V Creuze. 2016. Ocean One: A Robotic Avatar for Oceanic Discovery. In *IEEE Robotics Automation Magazine* 23, 4: 20–29. https://doi.org/10.1109/MRA.2016.2613281
19. Yong Jae Kim, Shanbao Cheng, Sangbae Kim, and Karl Iagnemma. 2012. Design of a tubular snake-like manipulator with stiffening capability by layer jamming. In *Proc. IROS 2012*, 4251–4256. https://doi.org/10.1109/IROS.2012.6385574
20. Yukari Konishi, Nobuhisa Hanamitsu, Kouta Minamizawa, Ayahiko Sato, and Tetsuya Mizuguchi. 2016. Synesthesia suit: the full body immersive experience. In *ACM SIGGRAPH 2016 VR Village*, 20. https://doi.org/10.1145/2945078.2945149
21. A. Kron, G. Schmidt, B. Petzold, M.I. Zah, P. Hinterseer, and E. Steinbach. 2004. Disposal of explosive ordnances by use of a bimanual haptic telepresence system. In *Proc. ICRA 2004*, 1968–1973. https://doi.org/10.1109/ROBOT.2004.1308112
22. Jaedong Lee, Youngsun Kim, and Gerard Kim. 2012. Funneling and saltation effects for tactile interaction with virtual objects. In *Proc. CHI 2012*, 3141. https://doi.org/10.1145/2207676.2208729
23. Richard Q der Linde, Piet Lammertse, Erwin Frederiksen, and B Ruiter. 2002. The HapticMaster, a new high-performance haptic interface. In *Proc. Eurohaptics 2002*, 1–5.
24. Michael A Liss and E M McDougall. 2013. Robotic surgical simulation. In *Cancer Journal (United States)* 19, 2: 124–129. https://doi.org/10.1097/PPO.0b013e3182885d79
25. Mariangela Manti, Vito Cacucciolo, and Matteo Cianchetti. 2016. Stiffening in soft robotics: A review of the state of the art. In *IEEE Robotics and Automation Magazine* 23, 3: 93–106. https://doi.org/10.1109/MRA.2016.2582718
26. Thomas H. Massie and J. K. Salisbury. 1994. The PHANTOM Haptic Interface : A Device for Probing Virtual Objects. In *Proceedings of the ASME Dynamic Systems and Control Division 1994*, 295-301.
27. Takashi Mitsuda, Sachiko Kuge, Masato Wakabayashi, and Sadao Kawamura. 2002. Wearable haptic display by the use of a Particle Mechanical Constraint. In *Proc. HAPTICS 2002*, 153–158. https://doi.org/10.1109/HAPTIC.2002.998953
28. Yusuke Nakagawa, Akiya Kamimura, and Yoichiro Kawaguchi. 2012. MimicTile : A Variable Stiffness Deformable User Interface for Mobile Devices. In *Proc. CHI 2012*, 745–748. https://doi.org/10.1145/2207676.2207782
29. Novint. Novint Falcon. Retrieved January 1, 2017 from http://www.novint.com/index.php/novintfalcon

30. Oculus. 2017. Oculus Rift. Retrieved from https://www.oculus.com/rift/
31. Oculus. 2017. Getting Started With Your Rock Band VR Connector. Retrieved from https://www.youtube.com/watch?v=HIEkqmmSWos
32. Angelika Peer and Martin Buss. 2008. A new admittance-type haptic interface for bimanual manipulations. In *IEEE/ASME Transactions on Mechatronics* 13, 4: 416–428. https://doi.org/10.1109/TMECH.2008.2001690
33. PJRC. 2017. Teensy USB Development Board. Retrieved January 1, 2017 from https://www.pjrc.com/teensy/index.html
34. ProTubeVR. 2017. ProTubeVR. Retrieved January 1, 2017 from https://www.protubevr.com/product-page/copie-de-protubevr-for-htc-vive-and-oculus-rift-inside-ue
35. Jukka Raisamo. 2010. Vibrotactile Movement and Its Applications for Virtual Reality. In *PIVE 2010*, 25-27.
36. Hitec RCD. 2017. HS-35HD Ultra Nano Servo. Retrieved January 1, 2017 from http://hitecrcd.com/products/servos/micro-and-mini-servos/analog-micro-and-mini-servos/hs-35hd-ultra-nano-servo/product
37. R. M. Sage. 1987. The mathematical modeling of ball joints with friction. Thesis. University of Leicester, Leicester, United Kingdom. http://hdl.handle.net/2381/34822
38. Jessie Lee C. Santiago, Isuru S. Godage, Phanideep Gonthina, and Ian D. Walker. 2016. Soft Robots and Kangaroo Tails: Modulating Compliance in Continuum Structures Through Mechanical Layer Jamming. In *Soft Robotics* 3, 2: 54–63. https://doi.org/10.1089/soro.2015.0021
39. Samuel B. Schorr and Allison M. Okamura. 2017. Fingertip Tactile Devices for Virtual Object Manipulation and Exploration. In *Proc. CHI 2017*, 3115–3119. https://doi.org/10.1145/3025453.3025744
40. Timothy M. Simon, Ross T. Smith, and Bruce H. Thomas. 2014. Wearable jamming mitten for virtual environment haptics. In *Proceedings of the 2014 ACM International Symposium on Wearable Computers*, 67–70. https://doi.org/10.1145/2634317.2634342
41. Christian Steins, Sean Gustafson, Christian Holz, and Patrick Baudisch. 2013. Imaginary devices: Gesture-based interaction mimicking traditional input devices. In *Proc. MobileHCI 2013*, 123. https://doi.org/10.1145/2493190.2493208
42. Anthony Talvas, Maud Marchal, Gabriel Cirio, and L Anatole. 2013. 3D Interaction Techniques for Bimanual Haptics in Virtual Environments. In *Multi-finger Haptic Interaction*, 31–53. https://doi.org/10.1007/978-1-4471-5204-0
43. Dzmitry Tsetserukou. 2011. FlexTorque, FlexTensor, and HapticEye: Exoskeleton Haptic Interfaces for Augmented Interaction. In *Proceedings of the 2nd Augmented Human International Conference*, 33:1--33:2. https://doi.org/10.1145/1959826.1959859
44. Dzmitry Tsetserukou, Shotaro Hosokawa and Kazuhiko Terashima. 2014. LinkTouch: A wearable haptic device with five-bar linkage mechanism for presentation of two-DOF force feedback at the fingerpad. In *Proc. HAPTICS 2014*, 307-312. https://doi.org/10.1109/HAPTICS.2014.6775473
45. B. Vanderborght, A. Albu-Schaeffer, A. Bicchi, E. Burdet, D. G. Caldwell, R. Carloni, M. Catalano, O. Eiberger, W. Friedl, G. Ganesh, M. Garabini, M. Grebenstein, G. Grioli, S. Haddadin, H. Hoppner, A. Jafari, M. Laffranchi, D. Lefeber, F. Petit, S. Stramigioli, N. Tsagarakis, M. Van Damme, R. Van Ham, L. C. Visser, and S. Wolf. 2013. Variable impedance actuators: A review. In *Robotics and Autonomous Systems* 61, 12: 1601–1614. https://doi.org/10.1016/j.robot.2013.06.009
46. VR Merch. 2017. HTC Vive Dual Controller Rifle Stock. Retrieved January 1, 2017 from https://vrmerch.com/products/htc-vive-dual-controller-rifle-stock
47. VR Merch. 2017. HTC Vive Golf Club Attachment. Retrieved January 1, 2017 from https://vrmerch.com/products/htc-vive-controller-golf-club
48. Ying Wei, Yonghua Chen, Yang Yang, and Yingtian Li. 2016. A soft robotic spine with tunable stiffness based on integrated ball joint and particle jamming. In *Mechatronics* 33: 84–92. https://doi.org/10.1016/j.mechatronics.2015.11.008
49. Kotaro Yamaguchi, Ginga Kato, Yoshihiro Kuroda, Kiyoshi Kiyokawa, and Haruo Takemura. 2016. A Non-grounded and Encountered-type Haptic Display Using a Drone. In *Proceedings of the 2016 Symposium on Spatial User Interaction*, 43–46. https://doi.org/10.1145/2983310.2985746
50. Vibol Yem and Hiroyuki Kajimoto. 2017. Wearable tactile device using mechanical and electrical stimulation for fingertip interaction with virtual world. In *Proc. IEEE Virtual Reality 2017*, 99-104. https://doi.org/10.1109/VR.2017.7892236